The Role of Bars in AGN Feeding

Luiz A. da Silva Lima[1]*, Lucimara Martins[1], Paula R. T. Coelho[2], Dimitri A. Gadotti[3], Geraldo Gonçalves[2]
1 Núcleo de Astrofísica, Universidade Cidade de São Paulo/ Universidade Cruzeiro do Sul. * luiz.sl@outlook.com
2 Instituto de Astronomia, Geofísica e Ciências Atmosféricas, Universidade de São Paulo.
3 Centre for Extragalactic Astronomy, Department of Physics, Durham University

INTRODUCTION

The AGN phenomenon is understood as the result of gas accretion by a supermassive black hole (M_{SMBH}) hosted in the central region of a galaxy. To sustain the observed luminosity, a mass on the order of $10^{5\text{-}6}$ $M_\odot$ should be accreted during the activity period. Therefore, a mechanism must be responsible for the transfer of angular momentum from the gas to allow its migration to the central region of a galaxy. The bar is one of the candidates for this mechanism. The non-axisymmetric potential of the bar promotes torques in the interstellar medium and momentum transfer, playing an important role in the secular evolution of a galaxy. In this work, we investigate the evidence for a connection between bars and AGN.

METHODOLOGY

We used the sample of galaxies studied by Gadotti (2009), obtained from the SDSS. The bar and galaxy properties were measured using BUDDA (Gadotti, 2008). The classification with respect to activity was done with BPT (Baldwin et al., 1981), where only AGN with higher luminosity were selected (Figure 1). Given a sample of barred galaxies and one of unbarred galaxies, the fraction of AGN between these two groups is one of the methods used to identify whether AGN are preferentially located in barred galaxies.

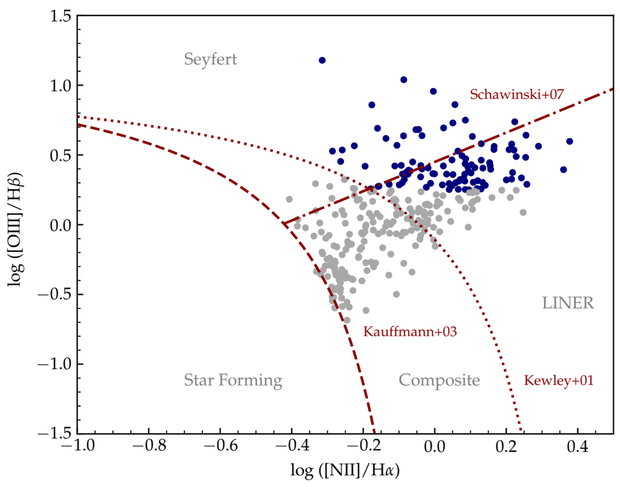

Figure 1. The BPT diagram, used for classifying objects based on their activity, reproduced from Silva-Lima et al. (2022).

One of the biggest challenges in these studies is the biases associated with sample selection. In an attempt to reduce bias, we utilized the MatchIt (Ho et al. 2007) code, based on propensity score matching (Rosenbaum and Rubin 1983), to construct our control sample of inactive galaxies. This approach enabled us to establish similar distributions of certain properties between the samples of active and inactive galaxies, with the aim of minimizing potential biases associated with these properties. Studies have found evidence that AGN are preferentially found in galaxies with higher stellar mass (M_*, e.g. Kauffmann et al. 2003). Additionally, properties of the bulge, such as its mass ($M_{*,\,bulge}$), exhibit a strong correlation with the mass of the supermassive black hole. A galaxy must also have gas available to be transported by the bar, and we employed colour as a proxy for estimating the gaseous content of a galaxy. Different values of the Sérsic index of the bulge can result from contrasting processes of bulge formation, including hierarchical and secular evolution. Furthermore, interaction with nearby galaxies can also trigger instabilities and redistribute momentum within a galaxy. In this case, we used the projected local density (Σ_5) to characterize the environment.

RESULTS

In the matching process, we used M_*, $M_{*,bulge}$, the colour, Σ_5, and the Sérsic index of the bulge in different combinations to select the quiescent galaxy samples and measure the AGN fraction. In all matching configurations, AGN were found to be preferentially located in barred galaxies (Figure 2).

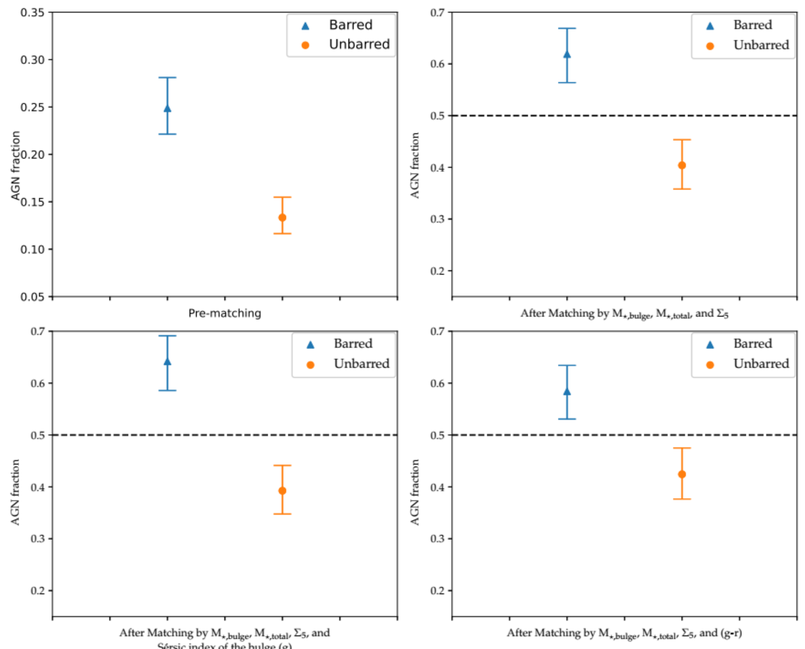

Figure 2. Fraction of AGN in barred and unbarred galaxies after matching with different parameters. Results show higher AGN fraction in barred galaxies. Reproduced from Silva-Lima et al. (2022).

We proceeded to explore the effect of a bar on the accretion rate (R) in AGN. M_{SMBH} was determined using the adjusted M-σ relation, considering morphological aspects (Graham et al., 2011). Our findings indicated that AGN in barred galaxies exhibit a higher accretion parameter R compared to those in unbarred galaxies. The Anderson-Darling test revealed a significant difference in the distribution of R (p-value ~ 0.004). It is important to note that when M_{SMBH} was determined using the M-σ relation without considering morphological differences, no significant differences in the accretion parameter R were observed.

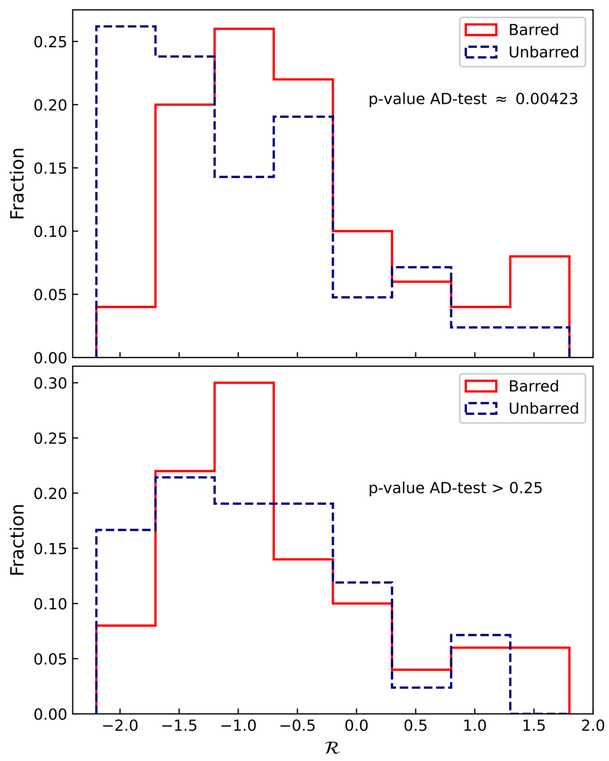

Figure 3. Distribution of the accretion parameter for barred and unbarred galaxies. Top panel: Considering morphology. Bottom panel: Using the same relation regardless of morphology. Reproduced from Silva-Lima et al. (2022).

In the last step of the analysis, we did not find correlations between parameters that estimate the bar strength and proxies of AGN activity. In Figure 4, we show one of these tests with ellipticity (Ɛ), boxiness (c) and Ɛ x c to estimate the bar strength against L[OIII], L[OIII] normalized by the luminosity of the SDSS 3'' fiber and R.

DISCUSSION

While we found AGN preferentially in barred galaxies where a difference in the R parameter was also observed, we did not observe a direct correlation between the bar strength and the intensity of the AGN. A possible explanation lies in the differences in the time scale of these processes and in the delays between the effects of the bar and the AGN manifestation. In this scenario, the gas transported by the bar is captured near the Lindblad resonance region, forming a reservoir. A secondary mechanism should then act to complete the accretion process.

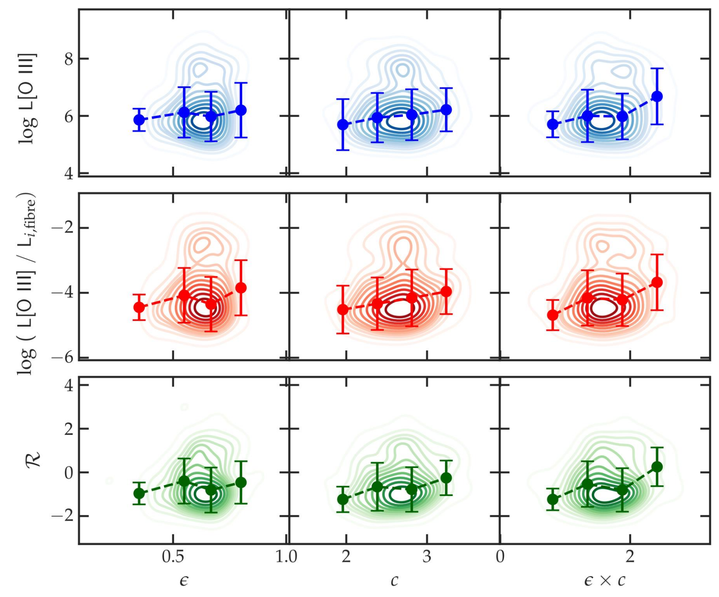

Figure 4. Comparison of parameters related to the strength of the bar in relation to activity tracer parameters.. Reproduced from Silva-Lima et al. (2022).

FUTURE WORKS

Studies of the central regions (~ 1 kpc) with integral field units (Gadotti et al. 2019) can help answer some of the questions related to the AGN feeding process.

We will build two samples of galaxies with AGN activity, one of them from barred galaxies and the other from unbarred ones. Thus, it will be possible to compare the physical properties and excitation mechanisms of nebular emission between these two populations. With this, we will try to answer the impact of the bars on star formation and gas dynamics in these central regions. We performed prospects for measuring emission lines and modeling the stellar population in the galaxy NGC 613, with TIMER observations (Gadotti et al. 2019).

We use a sequence of steps in a framework intended to optimize the masking of noisy regions of the spectral axis, measure and correct the dust attenuation in the stellar population, model the line-of-sight velocity distribution (LOSVD) with a 4th order Gauss-Hermite quadrature, and finally apply regularised fitting to model star formation history (Figure 5).

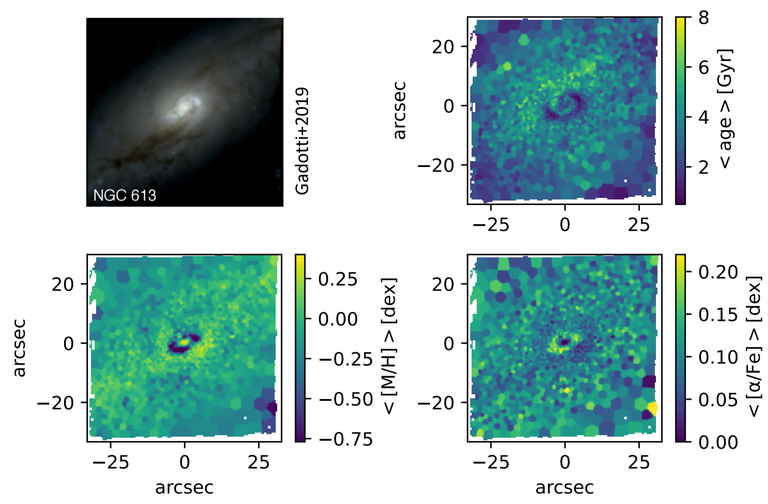

Figure 5. Stellar population properties. Top panel, left: NGC 613, reproduced from Gadotti et al. (2019); right: average stellar population age. Bottom, left: <[M/H]>; right: <[α/Fe]>.

We modelled the emission lines using multiple Gaussians to account for highly asymmetrical emission line profiles, arising from a combination of different gas excitation mechanisms. Additionally, we independently modelled high- and low-ionisation potential emission lines. This allows us to analyse the kinematics (Figure 6) and intensity of transitions, in order to identify the primary source of ionisation.

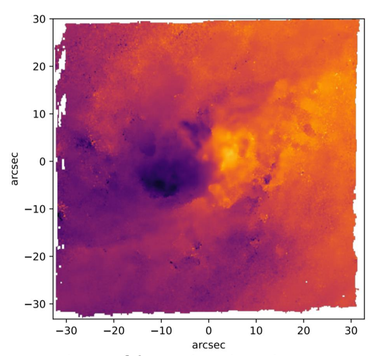

Figure 6. Gas kinematics of low-ionization potential lines.